Onset of magnetic order in $YbCu_{5-x}Al_x$

E. Bauer and R. Hauser
Institut für Experimentalphysik, Technische Universität Wien, A-1040 Wien, Austria

L. Keller and P. Fischer
Laboratorium für Neutronenstreuung, ETH Zürich and Paul Scherrer Institut, CH-5232 Villigen PSI, Switzerland

O. Trovarelli and J. G. Sereni
Centro Atomico Bariloche (CNEA), RA-8400 S.C. de Bariloche, Argentina

J. J. Rieger and G. R. Stewart
Inst. für Physik, Universität Augsburg, D-86135 Augsburg, Germany

(Received 12 December 1996)

Spectroscopic, magnetic, thermal, and transport measurements under pressure are presented which were performed on $YbCu_{5-x}Al_x$ intermetallics. The substitution of Cu by Al in $YbCu_5$ drives the system from an almost divalent behavior of the Yb ion in $YbCu_5$ to a trivalent state in $YbCu_3Al_2$. A compensation between the normal thermal expansion and a valence-driven contraction was found for $YbCu_4Al$. Antiferromagnetic order sets in for $x>1.5$, where an increasing Al content causes both a growing transition temperature and rising saturation moments reaching 2 K and about $2.1\mu_B$, respectively, for $x=2$. At the critical concentration ($x\approx1.5$) the possibility of a non-Fermi-liquid state is analyzed together with its tuning by pressure. [S0163-1829(97)03725-9]

I. INTRODUCTION

A substitution of Cu by Al or Ga in $YbCu_5$ offers the possibility to study the evolution of the ground-state configuration of the Yb ion in this hexagonal compound (space group $P6/mmm$) from the almost nonmagnetic $4f^{14}$ state ($YbCu_5$) to a magnetic $4f^{13}$ state in $YbCu_3Al_2$ or $YbCu_3Ga_2$.[1,2] This conclusion was drawn from various investigations of bulk properties performed on different samples of $YbCu_{5-x}M_x$ with $M=$ Al, Ga. In particular, it was shown that $YbCu_3Al_2$ exhibits even long-range antiferromagnetic order below ≈2 K.[1] The magnetic structure of this compound was already examined by means of elastic neutron scattering experiments, yielding a saturation moment of about $2.1\mu_B$/Yb for $T\rightarrow0$.[3] On the contrary, the Ga-based alloys remain paramagnetic down to 1.5 K. Concomitant with this observation is the fact that the valence ν of the compound richest in Ga does not attain the full integer valence limit ($YbCu_3Ga_2$, $\nu_{300\,K}\approx2.9$).[2] Negative logarithmic contributions to the electrical resistivity in the Al-based samples[1] as well as in the Ga-based materials under pressure,[2] enhanced values of the electronic contribution to the specific heat, or large thermopower values indicate that the Kondo effect is a predominant interaction mechanism within both series of alloys.

The aim of this paper is to present different experimental results allowing us to better understand the onset of magnetic order and to confirm the trivalent ground-state stabilization of the Yb ions upon the Cu/Al substitution. This evolution will be analyzed by a number of different investigations like the L_{III} absorption edge, elastic neutron scattering, ac and dc susceptibility, and specific heat measurements, and by a study of the pressure response of the electrical resistivity under hydrostatic pressures up to about 15 kbar.

At the onset of magnetic order for a critical concentration $x_0\simeq1.5$ the possibility of a non-Fermi-liquid behavior is analyzed, together with its tuning by applying pressure on one nonmagnetic sample.

II. EXPERIMENTAL DETAILS

The preparation of polycrystalline $YbCu_{5-x}Al_x$ samples with $0\leqslant x\leqslant2$ was already described in Ref. 1. To characterize the sample quality, both x-ray-diffraction and electron microprobe measurements were done for $x=1$, 1.5, and 2. While for $x=1$ indications of an impurity phase (consisting mainly of Cu_5Al) were observed, further increase of Al (i.e., $x=1.5$ and 2) stabilizes the expected $CaCu_5$ structure and the impurity phase completely vanishes.

X-ray-absorption spectroscopy (XAS) was carried out at the French synchrotron radiation facility (LURE) in Orsay using the x-ray beam of the DCI storage ring (working at 1.85 GeV and $\approx$320 mA) on the EXAFS D22 station. A double Si (311) crystal was used as a monochromator. Rejection of third-order harmonics was achieved with the help of two parallel mirrors adjusted to cut off energies higher than 10 keV. Experiments were carried out in the energy range 8080–9060 eV in order to study the L_{III} edge of Yb. Finely powdered samples were spread onto an adhesive Kapton tape and four such tapes were stacked together to prepare a sample layer of sufficient thickness to ensure a good signal. Moreover, this was also helpful to eliminate sample-free regions in the path of the radiation. The XAS spectra were measured at two fixed temperatures 10 K and 300 K.

Elastic neutron scattering experiments were done at the Saphir reactor of the PSI, Villigen, Switzerland, using the

double-axis multicounter neutron powder diffractometer DMC (Ref. 4) and the double-axis diffractometer P2AX. A ^{4}He cryostat was used to obtain temperatures down to 1.5 K, while a standard Oxford ^{3}He/^{4}He dilution refrigerator served to reach temperatures down to 10 mK. The powdered samples (about 20 g) were enclosed under a He gas atmosphere into cylindrical V tubes of 10 mm diameter and 50 mm height. For the dilution refrigerator experiments the samples were filled into a similar Cu container. The high-resolution mode was used employing a neutron wavelength $\lambda = 1.6984$ Å. The absorption-corrected neutron profile intensities were analyzed by means of a modified version of the Wiles-Young program. For investigation of magnetic ordering, neutron diffraction measurements were performed on the DMC in the high-intensity mode ($\lambda = 1.7034$ Å).

Bulk magnetization measurements in fields up to 8 T were carried out from $T = 1.5$ K up to room temperature using a standard extraction method. The low-field susceptibility values (shown in Fig. 4) were deduced from Arrott plots already presented in Ref. 1. A standard ^{3}He cryostat allowed ac susceptibility measurements with an excitation frequency of 128 Hz from 0.4 K to about 10 K.

Specific heat measurements on samples of about 2 g were performed at temperatures from 1.5 K up to 60 K by means of a quasiadiabatic step heating technique. Measurements down to 300 mK were carried out in a ^{3}He semiadiabatic calorimeter using the heat-pulse method and a three-wires Ge thermometry. Additionally, the heat capacity of a small piece (≈ 50 mg) of the alloy $YbCu_{3.25}Al_{1.75}$ (sample No. 2) was studied down to 300 mK using the time constant method.[5]

The electrical resistivity of bar-shaped samples was measured using a four-probe dc method in the temperature range from 1.5 K to room temperature. A liquid pressure cell with a 4:1 methanol-ethanol mixture as pressure transmitter served to generate hydrostatic pressure up to about 15 kbar. The absolute value of the pressure was determined from the superconducting transition temperature of lead.[6]

III. RESULTS AND DISCUSSION

A. L_{III} absorption edge measurements

Since the magnetic state of Yb systems is intimately connected with the valence state of the Yb ions, L_{III} absorption edge measurements were done at two different temperatures in order to evaluate the thermal stability of the Yb valence in $YbCu_{5-x}Al_x$. Figure 1 shows results of such measurements performed at $T = 10$ K and 300 K, respectively. These measurements unambiguously indicate a concentration-dependent shift of spectral weight from the nearly divalent state of Yb in $YbCu_5$ to the trivalent state of Yb as $YbCu_3Al_2$ is approached. Additionally, there is also a weak temperature dependence of the valence state in some of these alloys, which is considered to be characteristic of intermediate valence materials. To establish the relative weight of both electronic configurations, the spectra were decomposed into a pair of Lorentzians and modified inverse tangent functions.[2] Based on least squares fits of these functions to the data, the valence ν of the Yb ions in the different alloys was evaluated. Figure 2 represents results of these analyses for all concentrations investigated for 10 K and 300 K, respectively. In contrast to an almost 2+ state which was concluded from susceptibility measurements by Iandelli and Palenzona,[7] the present L_{III} measurements on $YbCu_5$ indicate a valence of $\nu \approx 2.3$ at room temperature which does not change as the temperature is lowered. As the Al content increases, the valence ν of Yb ions starts to rise. A 3+ state is approached for $x > 1.5$ where the valence appears to be temperature independent. One has to note that the valence dependence on temperature for $x = 0.75$ and 1.0 indicates that the energy difference (E_{ex}) between the Yb^{3+} and the Yb^{2+} electronic configurations (EC's) is of the order of the thermal excitation energy ($\simeq 300$ K), whereas for $x = 0$ and for $x \geqslant 1.5$ the difference of the EC's is much larger and consequently no valence change is observed in the temperature range investigated. For concentrations $x = 0.75$ and $x = 1$, it follows that the Yb^{2+} configuration is the one with lower energy because ν increases with temperature, though even in case of $x = 0$, the noninteger value of ν denote a

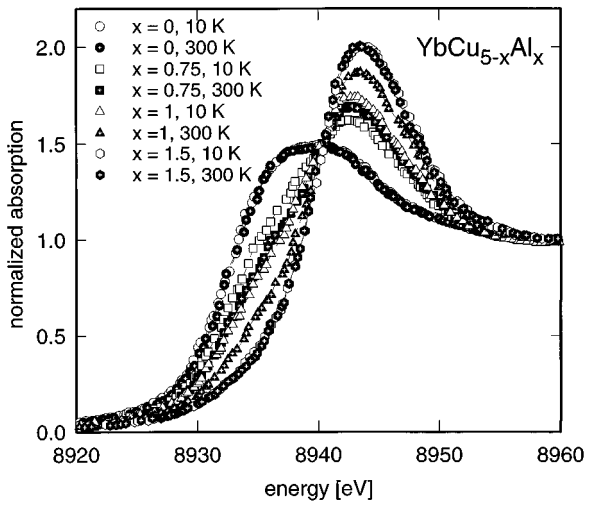

FIG. 1. X-ray absorption as a function of energy of $YbCu_{5-x}Al_x$ at $T = 10$ and 300 K.

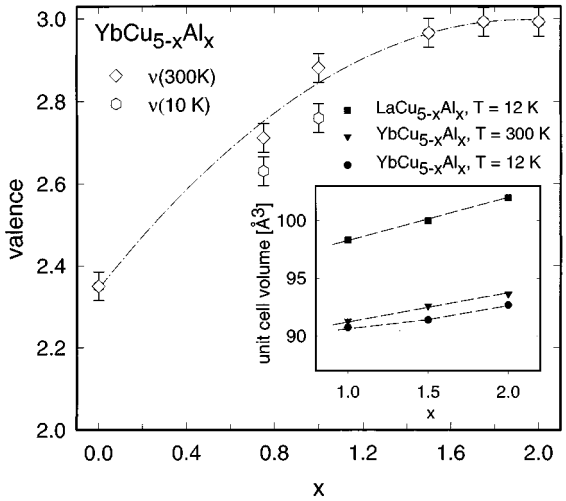

FIG. 2. Concentration and temperature dependent valency ν of $YbCu_{5-x}Al_x$. The dash-dotted line is a guide for the eyes. The inset shows the concentration-dependent unit cell volume of $YbCu_{5-x}Al_x$ (at $T = 12$ K and 300 K) and of the isomorphous nonmagnetic series $LaCu_{5-x}Al_x$.

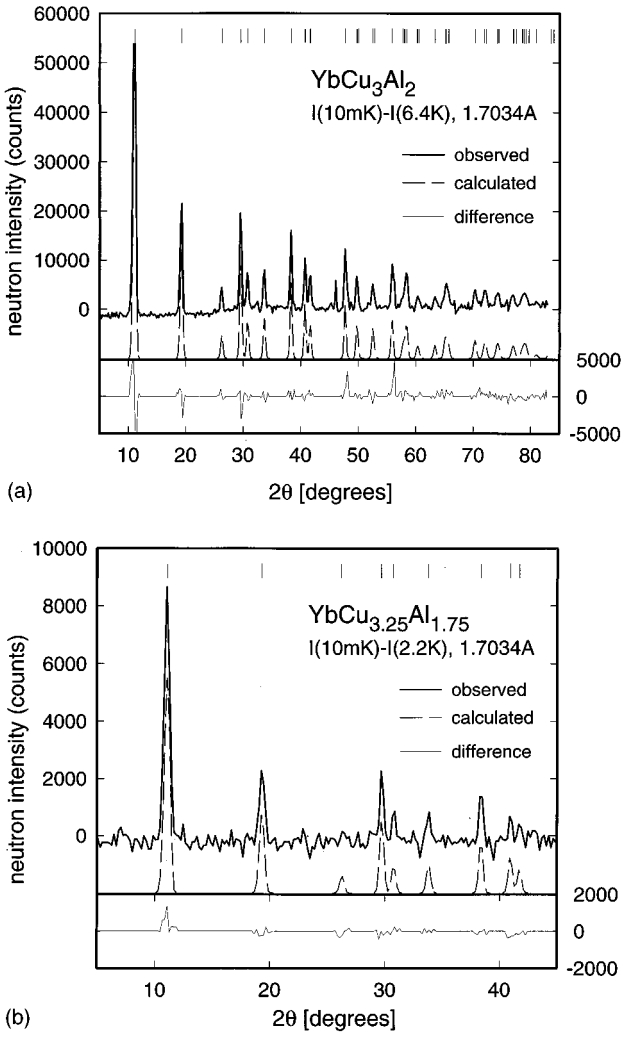

FIG. 3. Magnetic difference neutron diffraction pattern I (10 mK)–I (6.4 K) and I (10 mK)–I (2.2 K) of antiferromagnetic $YbCu_3Al_2$ (a) and $YbCu_{3.25}Al_{1.75}$ (b), respectively.

weak mixture between both configurations. Since the Cu/Al substitution does not cause a change of the crystal structure, but an increase of the volume of the unit cell (see inset of Fig. 2), one would expect to favor the Yb^{2+} configuration with the larger ionic volume as x increases. However, as discussed later, the increase of the number of electrons in the conduction band of the system appears to be the dominant effect.

B. Magnetic properties

1. Elastic neutron scattering experiments

The difference diagrams of the neutron scattering intensities measured at $T=10$ mK and $T=2.2$ K and 6.4 K for $YbCu_3Al_2$ and $YbCu_{3.25}Al_{1.75}$ are shown in Figs. 3(a) and 3(b), respectively. Both compounds exhibit additional Bragg peaks below the magnetic phase transition temperature, indicating antiferromagnetic order. Since the magnetic intensity for the latter alloy is much weaker compared to that of $YbCu_3Al_2$, the peaks of magnetic origin above about $2\theta \approx 40°$ vanish in the background and are therefore skipped in Fig. 3(b). However, a comparison of the observed peak and intensity distribution of both compounds corroborates similar crystal and magnetic structures.

Since the structural unit cell contains only one Yb atom, each type of antiferromagnetic structure is responsible for an enlarged magnetic unit cell. A Rietveld analysis of the position and the intensities of the magnetic Bragg peaks points to an antiferromagnetic structure with a propagation vector of $\vec{k}=(1/2,1/2,0)$. Along the $\vec{c}$ axis, all the Yb moments are aligned ferromagnetically. Both the propagation vector and the moment alignment do not change with Al concentration. The best fit is achieved for moments parallel to the $\vec{c}$ axis with $\mu_{Yb}=2.10(5)\mu_B$ in the case of $YbCu_3Al_2$ and $\mu_{Yb}=1.18(2)\mu_B$ in the case of $YbCu_{3.25}Al_{1.75}$.

The crystal field (CF) with hexagonal symmetry causes the eightfold degenerate ground state (GS) of the Yb moment to be lifted into four doublets $\Gamma_7=|\pm 1/2\rangle$, $\Gamma_9=|\pm 3/2\rangle$, $\Gamma_{8a}=\alpha|\pm 5/2\rangle+\beta|\pm 7/2\rangle$, and $\Gamma_{8b}=\beta|\mp 7/2\rangle+\alpha|\pm 5/2\rangle$, with the respective moments along the $\vec{c}$ direction obtained from $\mu_c=g_j\mu_B\langle\Gamma_i|J_z|\Gamma_i\rangle$. Assuming Γ_7 or Γ_9 as a possible CF GS, the calculated moments are $0.57\mu_B$ and $1.71\mu_B$, respectively, which are smaller than the ones observed for $YbCu_3Al_2$. Consequently, the Γ_7 or the Γ_9 doublet can be excluded from being the GS in $YbCu_3Al_2$; by analogy this should hold also for $YbCu_{3.25}Al_{1.75}$. Such a conclusion also applies to isothermal magnetization results[1] and is confirmed from recent low-temperature Mössbauer spectroscopy data of $YbCu_3Al_2$.[8] Depending on the value of α and β, the moment associated with the Γ_{8a} and the Γ_{8b} doublet ranges between $2.85\mu_B$ and $4\mu_B$. Thus the observed values of the saturation moments are in any case substantially reduced to a maximum value of $2.1\mu_B$/Yb for $x=2$. In accordance to the previously studied transport properties and the entropy evolution of the ordered phase of $YbCu_{5-x}Al_x$ (shown in the inset of Fig. 5), Kondo interaction seems to be responsible for this reduction. The results observed from the neutron scattering study indicate that the Cu/Al substitution favors the development of magnetic order, with a consequent increase of the spontaneous magnetic moment.

2. Magnetic susceptibility

The temperature dependence of the inverse magnetic susceptibility χ^{-1} of $YbCu_{5-x}Al_x$ is displayed in Fig. 4 for $x=1$, 1.5, and 2. The inset shows $\chi(T)$ of $x=1.5$, 1.75, and 2 at low temperatures. This susceptibility data reflect the onset of magnetic order at 1.05 K and 2 K for $x=1.75$ and $x=2$, respectively. No order down to 0.4 K is observed for $x=1.5$. As already indicated in a previous paper,[1] $\chi(T)$ data of $x=1.5$ and $x=2$ can be described above ≈ 50 K by a Curie-Weiss law, i.e., $\chi(T)=\chi_0+C_c/(T+\theta_p)$, with χ_0 a temperature-independent Pauli susceptibility contribution, C_c the Curie constant, and θ_p the paramagnetic Curie temperature. The results of least squares fits are indicated in Table I. Although the deviation of $\chi^{-1}(T)$ from the Curie-Weiss behavior below 50 K for the $x=2$ sample may be ascribed to CF splitting, in the case of $x=1.5$, the Kondo effect or magnetic fluctuations should play a more important role as will be discussed later.

For $x=1$, a crude approximation according to $\chi(T)=C_c/(T+\theta_p)$ and $T>100$ K gives values of $\mu_{eff}\approx 4.7\mu_B$ and $\theta_p\approx -350$ K. However, due to the slightly

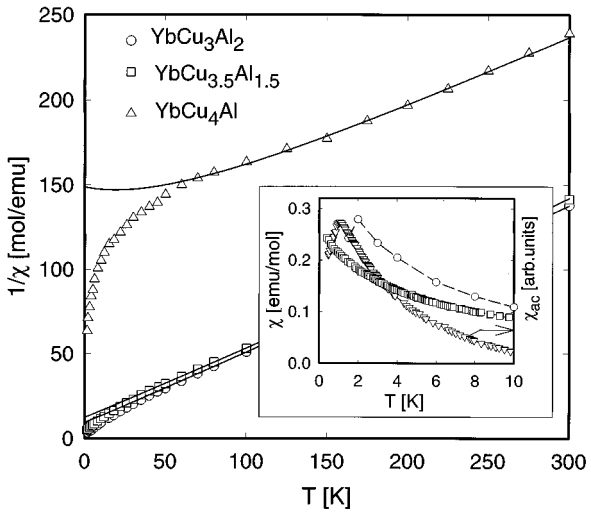

FIG. 4. Temperature-dependent magnetic susceptibility χ of $YbCu_{5-x}Al_x$ compounds plotted as χ^{-1} vs T. The solid lines are least squares fits according to the ICF model. The inset shows the low-temperature magnetic susceptibility for $x=1.5$, 1.75, and 2.

positive curvature of $\chi^{-1}(T)$ at high temperatures, that assumption does not describe properly the experimental data. Therefore, a model accounting for the noninteger valence of the Yb ion has to be used. A phenomenological description of such a situation is provided by the interconfiguration fluctuation model (ICF).[9] This model evaluates $\chi(T)$ as the result of the two EC contributions (Yb^{3+} and Yb^{2+} in this case), taking into account their respective thermal occupation weight. There, the usual Curie-Weiss law is simply modified by considering the Curie constant as temperature dependent, $C(T)=C_c n_f(T)$, with

$$n_f(T)=\frac{8}{8+\exp[-E_{\rm ex}/k_B(T+T_{\rm sf})]}, \qquad (1)$$

where $E_{\rm ex}$ is the energy difference between both EC's with respective degeneracies 8 and 1, and $T_{\rm sf}$ is proportional to the fluctuation frequency among them. For practical purposes, the energy scale of $T_{\rm sf}$ resembles the Kondo temperature T_K.

Least squares fits to the susceptibility data according to this model are shown as solid lines in Fig. 4. Since magnetic impurities ($x=1$) or CF effects ($x=2$) may become significant below ≈ 50 K, the fits were performed above that temperature. The obtained parameters are collected in Table I. The large negative value of $E_{\rm ex}$ evaluated for $YbCu_4Al$ in fact indicates that the magnetic $4f^{13}$ state is situated well above the nonmagnetic $4f^{14}$ ground state. A typical Curie-Weiss behavior is therefore expected only at considerably higher temperatures. On the other hand, the same analysis performed on $YbCu_{3.5}Al_{1.5}$ and $YbCu_3Al_2$ yields an inverse situation; i.e., positive values of $E_{\rm ex}$ reflect that the magnetic $4f^{13}$ configuration is the GS, resulting in a Curie-Weiss-like behavior. The valence of $YbCu_{5-x}Al_x$ can subsequently be evaluated by $\nu(T)=2+n_f(T)$; see Table I. The coincidence between the ν values obtained from $L_{\rm III}$-XAS experiments and those evaluated by applying the ICF phenomenological model to $\chi(T)$ is remarkable despite the fact that CF effects were not taken into account. A further analysis of the $\chi^{-1}(T)$ data of $YbCu_{3.5}Al_{1.5}$ at low temperatures (cf. Fig. 7) indicates that certain magnetic interactions are present at that concentration because the best fit obtained up to 50 K follows a power law with an exponent close to 2/3 instead of 1 (expected from the usual Curie-Weiss law).

Taking $T_{\rm sf}$ as a measure of the mixture of both Yb electronic configurations, the values extracted from the respective fittings (see Table I) indicate that the significant mixture observed for $YbCu_4Al$ becomes negligible for $x \geqslant 1.5$.

C. Thermal properties

The temperature-dependent specific heat C_p of $YbCu_{5-x}Al_x$ for $x=1.5$, 1.75, and 2 is shown in Fig. 5. The $C_p(T)$ for $x=1.75$ was studied on samples from two different batches. While $C_p(T)$ of sample No. 1 was measured on the usual bulk material, $C_p(T)$ of No. 2 was obtained on a powdered and subsequently pressed specimen which was also used for the neutron scattering experiments. $C_p(T)$ of both $x=1.75$ and $x=2$ show anomalies at $T\approx 1$ K and

TABLE I. Néel temperature T_N, saturation moment $\mu_{\rm Yb}$, effective magnetic moment $\mu_{\rm eff}$, paramagnetic Curie temperature θ_p, valence obtained from the $L_{\rm III}$ spectra at 300 K $\nu_{300\,\rm K}$, energy difference between the $4f^{14}$ and the $4f^{13}$ state of the Yb ion $E_{\rm ex}$, fluctuation temperature $T_{\rm sf}$, and valency deduced from the ICF model, $\nu^*_{300\,\rm K}$.

$YbCu_{5-x}Al_x$	$x=1$	$x=1.5$	$x=1.75$	$x=2$
T_N [K]	—	—	1.05	2.0
$\mu_{\rm Yb}$ [μ_B/Yb]	—	—	1.18(2)	2.10(5)
$\mu_{\rm eff}$ [μ_B/Yb]	no CW[a]	4.28	n.d.[b]	4.3
θ_p^c [K]	≈ -350[c]	-22	n.d.[b]	-17
$\nu_{300\,\rm K}$	2.85	2.97	2.99	2.99
$E_{\rm ex}/k_B$ [K]	-390	530	n.d.[b]	660
$T_{\rm sf}$ [K]	170	20	n.d.[b]	18
$\nu^*_{300\,\rm K}$	2.78	2.93	n.d.[b]	2.95

[a]No Curie-Weiss behavior.
[b]Not determined.
[c]Obtained from a high-temperature extrapolation.

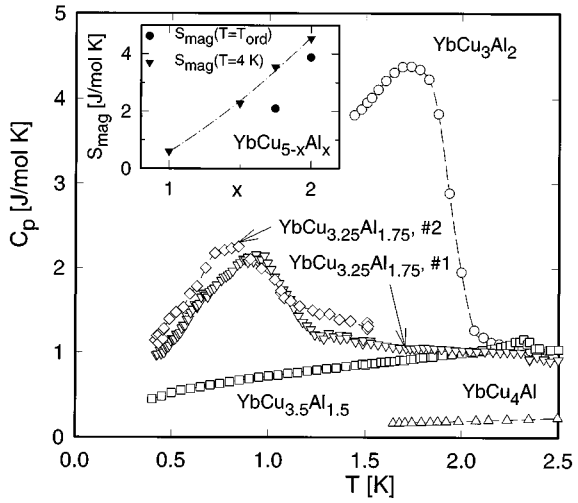

FIG. 5. Temperature-dependent specific heat C_p of various $YbCu_{5-x}Al_x$ alloys. The inset shows the concentration dependence of the magnetic entropy depicted at $T=T_N$ and at $T=4$ K.

$T\approx 2$ K, respectively, indicating the onset of long-range magnetic order. The thus-deduced transition temperatures agree well with the data observed from the susceptibility measurements of the previous section. In the $x=1.5$ sample, an anomaly in the vicinity of 2.3 K originates from a small amount of magnetically ordered Yb_2O_3. The height of the specific heat jump at T_N, δ_{C_p}, increases with increasing Al content. The observed broadened phase transition indicates short-range-order effects above the transition temperature, partially intrinsic and partially due to the polycrystalline character of the samples. Nevertheless, the concentration-dependent increase of $\delta_{C_p}(x)$ seems to overcome these effects, indicating a decrease of $T_K(x)$ as the primary mechanism for such a variation, in agreement with theoretical predictions[10] and transport properties such as resistivity and thermopower.[1] Within that pattern[10] the experimental data yield $T_K\approx 4$ K and 3 K for $YbCu_{3.25}Al_{1.75}$ and $YbCu_3Al_2$, respectively. The magnetic entropy gain S_{mag} of this system at $T=T_N$ and at 4 K (inset, Fig. 5) is concomitant with this tendency. Although the expected entropy of $R\ln 2$ for a doublet GS is not reached, there is a clear tendency towards that value as the Al content increases.

Remarkably large values of the electronic contribution to the specific heat are found for some concentrations of this series. A value of more than 1 J/mol K^2 is approached by $YbCu_{3.5}Al_{1.5}$ if C_p/T is extrapolated towards zero. This value contrasts with the observed one for $YbCu_4Al$ (0.05 J/mol K^2) representing the intermediate valence (IV) behavior of this alloy system. On the other hand, C_p/T of $YbCu_{3.25}Al_{1.75}$ attains about 2 J/mol K^2 (depending on the extrapolation criterion), despite this alloy exhibiting a magnetically ordered GS.

D. Pressure response of the electrical resistivity

Previous studies showed already that pressure applied to Yb-based compounds is responsible for the stabilization of the $4f^{13}$ state of the Yb ion.[11] This follows from the fact that the atomic radius of the nonmagnetic $4f^{14}$ state is larger than

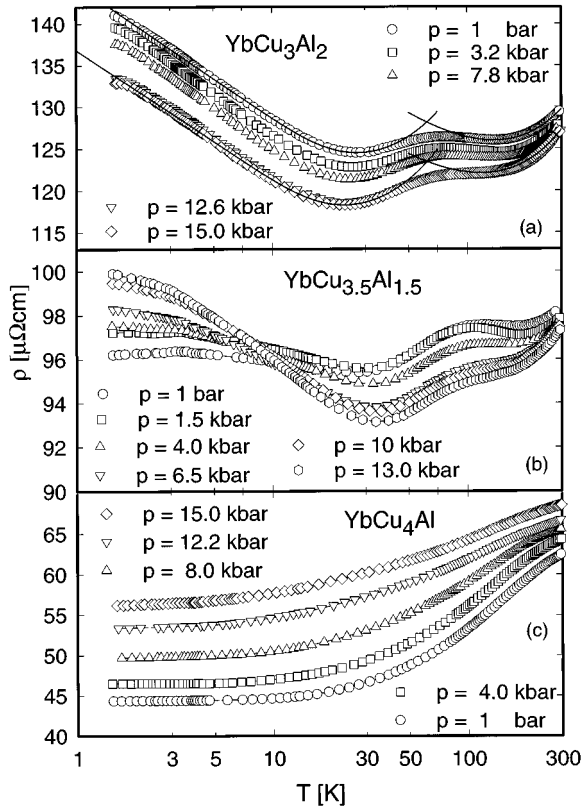

FIG. 6. Temperature- and pressure-dependent electrical resistivity ρ of $YbCu_{5-x}Al_x$: (a) $x=2$, (b) $x=1.5$, and (c) $x=1$.

that of the magnetic $4f^{13}$ state. Thus, a reduction of volume by pressure is expected to favor the magnetic configuration. Figure 6 shows the pressure- and temperature-dependent resistivity of $YbCu_{5-x}Al_x$ for $x=2$, 1.5, and 1.

It is important to note that the residual resistivity of this series at ambient pressure increases with increasing Cu/Al substitution. This seems to be correlated, at least partly, with the growing crystallographic disorder, since Al replaces Cu statistically at the $3(g)$ sites of the $CaCu_5$ structure.

Starting from the magnetic side, the most striking feature observed for $YbCu_3Al_2$ under pressure is the almost ''parallel'' decrease of the absolute resistivity in the low temperature range [Fig. 6(a)]. Above that range, local maxima in the vicinity of 70 K are shifted slightly to higher temperatures. Well below and above these maxima, the temperature-dependent resistivity can be accounted for in terms of the residual resistivity, electron-phonon interaction, and by the negative logarithmic Kondo term, as proposed in Ref. 1, i.e., $\rho(T)=\rho_0+\rho_{\mathrm{ph}}(T)+\rho_K(T)$. The results of least squares fits at high and at low temperatures for two values of pressure are shown as solid lines in Fig. 6(a). The reasonable agreement between the theoretical prediction and experimental data confirms the Kondo interaction to be present in this compound. According to a model of Cornut and Coqblin,[12] the particular behavior of the magnetic contribution to the electrical resistivity, ρ_m, arises from the competition between CF splitting and Kondo effect. The negative logarithmic behavior at low and high temperatures reflects the Kondo effect in the CF ground state and the excited levels of the Yb ion, respectively, whereas the maximum of ρ_m is roughly a measure of the overall CF splitting (Δ_{CF}). The

slight shift of the local maximum in $\rho(T)$ to higher temperatures as the pressure increases can be understood in terms of the simple point-charge model. As already indicated, the negative logarithmic slope of the resistivity in the crystal field ground state appears to be unchanged as the pressure varies. According to Ref. 12, the slope of $\rho_m(T)$ depends on $J^3N(E_F)^2$, where J is the s-f coupling constant and $N(E_F)$ is the electronic density of states at the Fermi energy. Since T_K of Yb systems decreases with applied pressure[11] and furthermore since $T_K \propto \exp[-1/(|J|N(E_F)]$, a decrease of the slope would be expected too. However, the observed behavior is in contradiction to this model. It is therefore supposed that, at least, additional parameters of that model have to be taken into consideration in order to get an appropriate description of the pressure dependent changes in $YbCu_3Al_2$.

From a more phenomenological point of view, the peculiarities of the pressure response $\Delta\rho(p,T)$ $[\Delta\rho(p,T)=\rho(p,T)-\rho(p=1\text{bar},T)]$ of $YbCu_3Al_2$ can be understood from a different pressure impact at low and at high temperatures. While $\Delta\rho(p,T)$ in the low-temperature region is almost temperature independent, a clear temperature dependence is observed above 20 K, i.e., in a temperature region where the occupancy of the excited crystal field levels becomes important. Two effects can contribute to such a $\Delta\rho(p,T)$ dependence: (i) an increase of crystal field splitting due to the pressure-driven decrease of the interatomic lattice spacing and therefore an approaching of the ionic charges and (ii) a narrowing of the CF levels because hybridization in Yb systems is expected to decrease with pressure. Such a mechanism obviously would cause a reduction of scattering, more pronounced at low temperatures, and in turn a smaller resistivity would result. In contrast to well-studied Ce-based Kondo systems, e.g., $CeAl_2$,[13] the overall pressure response of $YbCu_3Al_2$ appears to be mirrorlike in the pressure and temperature range covered.

Passing over to the IV limit (i.e., $YbCu_4Al$) the pressure response appears to be completely different; see Fig. 6(c). In this case $\rho(T)$ increases in the whole temperature range under pressure. Moreover, $\rho(T)$ of $YbCu_4Al$ at normal pressure exhibits a T^2 behavior at low temperatures as is expected for a Fermi-liquid system, but the exponent decreases with increasing pressure to become close to unity at $p \approx 15$ kbar. It can be expected that, as the valence of the Yb ion increases with pressure, magnetic interactions gain weight, because the magnetic $4f^{13}$ state is progressively approached. Consequently, magnetic scattering of the conduction electrons on the Yb moments becomes much more important, and hence the resistivity values become larger.

The temperature-dependent resistivity and the pressure response of $YbCu_{3.5}Al_{1.5}$ [Fig. 7(b)] appears to be roughly between both former cases. At ambient pressure, the total temperature-dependent variation of $\rho(T)$ (between 1.5 and 300 K) does not exceed 2.5 $\mu\Omega$ cm, less than one-tenth of the total variation of $x=1$ and $x=2$ samples. Local maxima in the vicinity of 100 K indicate the crystal field splitting. The striking feature of the $\rho(T,p)$ dependence at this Al concentration is the increase of the low-temperature resistivity (like for $x=1$) while above about 50 K it decreases (like for $x=2$). Such an apparently ambiguous behavior can be understood taking at first into account that T_{sf} (or T_K) becomes smaller than Δ_{CF}, allowing for an independent behavior of the ground and excited CF levels. Then, if the elastic energy provided by the applied pressure is compared with the thermal energy, one would expect that the latter will exceed the former at a certain temperature, which in this case appears to be smaller than the Δ_{CF} value. In other words, there are magnetic correlations related to the GS energy scale that can be driven by $p=13$ kbar, whereas such a perturbation will only produce a slight shift in the excited CF energy levels. We note that the change of the pressure response from an increase of $\rho(T)$ to a decrease, observed roughly at $T \simeq 10$ K, appears to be similar to the energy shift of the excited CF levels.

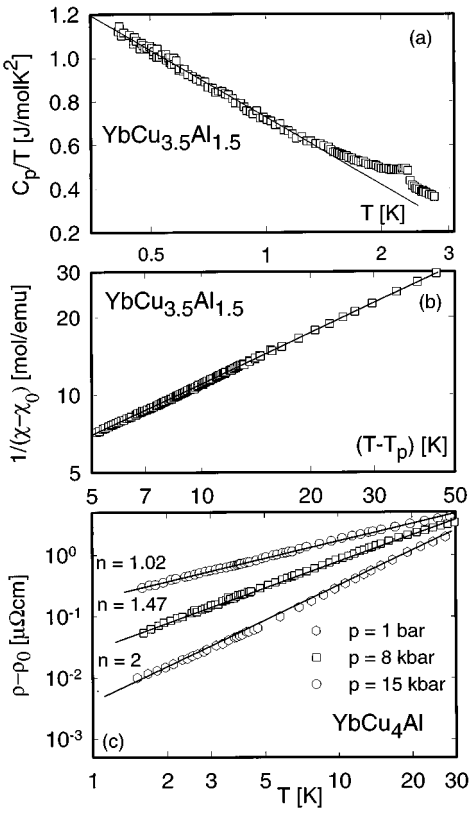

FIG. 7. Logarithmic temperature dependence of C_p/T: χ^{-1} of $YbCu_{3.5}Al_{1.5}$ and $\rho_m(T,p)$ of $YbCu_4Al$.

IV. DISCUSSION

Two driving forces compete in the evolution of the magnetic properties of $YbCu_{5-x}Al_x$. One is the increase of the number of electrons in the band originating from the substitution of a single-electron element (Cu) by a three-electron one (Al). This growing electron number is assumed to be responsible for the observed valence change throughout this series. The other one is the enlargement of the volume of the unit cell produced by the difference between the atomic sizes of Cu and Al. Because the volume of the nonmagnetic Yb^{2+} configuration is larger than that of the magnetic Yb^{3+} one, both effects should be opposite. Within such a panorama, some striking features like the significant $\nu(T)$ dependence for $x=0.75$ and 1 may occur to be in contrast to a constant value of $\nu(T)$ observed for $x=0$ and $x \geqslant 1.5$.

The particular behavior of $\nu(T)$ of $YbCu_{5-x}Al_x$ influ-

ences also the usual thermal expansion of the unit cell (inset, Fig. 2). While for the stable valence regime ($x \geqslant 1.5$) a volume change $\Delta V/V$ between room temperature and 12 K of more than 1% is observed, $\Delta V/V$ of $x=1$ amounts just to about 0.5%. There, the increase of V with increasing temperature is partly compensated by the decrease in volume associated with the change in valence on heating. Additional evidence for such a volume contraction due the valence change can be found at $T=12$ K from the $V(x)$ slope which changes as the Yb ion tends to the 3+ state (cf. inset, Fig. 2). In contrast, $V(x)$ of the reference series $LaCu_{5-x}Al_x$ at $T=12$ K shows a much steeper and almost constant slope.

The evolution of $\nu(x)$ as observed from the L_{III} spectra is confirmed by the crossover from an almost-temperature-independent Pauli susceptibility in $YbCu_5$ to a Curie-Weiss behavior in the case of $YbCu_3Al_2$, which is accompanied by a substantial reduction of the absolute value of the paramagnetic Curie temperature $|\theta_p|$ from about -350 K for alloys near to $YbCu_4Al$ to a value of about -20 K for alloys near to $YbCu_3Al_2$. In the scope of the Kondo picture, $|\theta_p|$ is proportional to T_K;[14] thus, as T_K decreases the screening of the Yb moments becomes weaker and long-range magnetic order gets possible. A similar description applies to T_{sf}.

Concerning pressure effects, contrary to Ce compounds, the resistivity of stable valent $YbCu_3Al_2$ decreases as the pressure rises [cf. Fig. 6(a)]. However, within the unstable valent region the effect is reversed because pressure favors the smaller Yb^{3+} magnetic EC's, which enhances the magnetic electronic scattering [cf. Fig. 6(c)].

When $Yb(Cu,Al)_5$ and $Yb(Cu,Ga)_5$ ground states are compared, a sort of shift in the magnetic properties is evidenced. While the former exhibits long-range magnetic order, the latter series seems to stay paramagnetic.[2] This qualitative difference appears to be correlated with the valence of the respective alloys: Only systems in both series with ν very close to 3+ are able to form a long-range-ordered ground state. This condition is proved just for the Al-based alloys beyond $x>1.5$, while the Ga-based series at ambient pressure and at room temperature does not exceed a valence of about 2.9. In this context it should be noted that for the isomorphous cerium series, i.e., $Ce(Cu,Al)_5$ and $Ce(Cu,Ga)_5$, the more ''magnetic'' state is observed for the Ga-based alloys.[15] However, it is ambiguous whether this difference of the hybridization strength between Al and Ga, on the one hand, as well as Ce and Yb, on the other hand, is only a consequence of the electron-hole symmetry. Under pressure, L_{III} XAS measurements up to 175 kbar indicate that the Yb valence in $YbCu_4Ga$ increases from 2.57 ($p=1$ bar) to 2.96 ($p=175$ kbar).[16] Since at ambient pressure ν of $YbCu_4Al$ is much larger than $YbCu_4Ga$, a smaller value of pressure should be sufficient to obtain for this alloy the magnetic 3+ state.

Various investigations were recently devoted to Kondo systems at the verge of the onset of magnetic order,[17] which can be considered as candidates for the so-called non-Fermi-liquid (NFL) behavior. In order to examine whether $YbCu_{5-x}Al_x$ at $x=1.5 \simeq x_0$ is also characterized by such a behavior, the present $C_p/T(T)$ results were plotted as $f(\ln T)$ in Fig. 7(a). In this case, there is a clear tendency to a logarithmic temperature dependence, which is considered as a sign of a NFL-type state. A tentative fit below ≈ 1.5 K according to $C_p/T = a\ln(T/T_0)$ yields a logarithmic divergence ($a<0$) and the characteristic temperature $T_0 \approx 6$ K [solid line in Fig. 7(a)]. At this concentration of the series, signs for NFL behavior were also found from the temperature-dependent magnetic susceptibility by a power law according to $1/\chi = a(T+T_p)^{2/3} - b$ (up to $\simeq 50$ K), where a, T_p, and b are constants [Fig. 7(b)]. To our knowledge, at present there is not a model proposing a $T^{-2/3}$ dependence for $\chi(T)$; however, the divergent character of both $\chi(T)$ and $C_p/T(T)$ at low temperatures clearly places $YbCu_{3.5}Al_{1.5}$ into the group of those systems which cannot be described as usual Fermi liquids.

Complementary information is found from the pressure effect on the $[\rho(T)-\rho_0] \propto T^n$ dependence of $YbCu_4Al$, which is shown in Fig. 7(c) in a double-logarithmic representation. There, the evolution of $n=f(p)$ is clearly evidenced as a decrease of the exponent n ($n=2$, 1.47, and 1.02 for $p=1$ bar, 8 kbar, and 15 kbar, respectively). While $n=2$ represents a typical Fermi liquid at ambient pressure, values with $n<2$ for increasing pressures may be interpreted as a breakdown of the Fermi-liquid ground state. Exponents similar to that found for $YbCu_4Al$ ($n \approx 1.5$ at 8 kbar) were already calculated theoretically for non-Fermi-liquid systems, e.g., in the scope of a generalized scaling theory of heavy fermions,[18] by an interplay of disorder and correlations yielding to a distribution of Kondo temperatures[19] or by using a sum rule to account for spin fluctuations around their antiferromagnetic instability.[20]

V. SUMMARY

The present investigations on the series $YbCu_{5-x}Al_x$ show the onset of long-range magnetic order due to the Cu/Al substitution, with a simultaneous growth of T_N and the magnitude of the saturation moments for concentrations $x>1.5$ as the Yb^{3+} electronic configuration stabilizes. The valence evolution of the Yb ion due to the Cu/Al substitution is also reflected in the effect of pressure on the electrical resistivity, which makes possible to distinguish the difference between the ground and excited CF levels in the particular case of $YbCu_{3.5}Al_{1.5}$. At the intermediate valence region, a compensation of the usual thermal expansion and the Yb valence driven contraction is observed. The series selected is also an example for a crossover of the regimes from high ($YbCu_5$) to low Kondo temperatures ($YbCu_3Al_2$). In the proximity to the onset of magnetic order (i.e., $x=x_0=1.5$) some hints for non-Fermi-liquid behavior are observed. There, the low-temperature specific heat of $YbCu_{3.5}Al_{1.5}$ follows a $C_p/T \sim \ln(T/T_0)$ dependence and the decrease of the temperature exponent of the $\rho(T)$ of $YbCu_4Al$ recalls the ''tuning'' of this behavior in $CeCu_{6-x}Au_x$.[21]

ACKNOWLEDGMENTS

Parts of this work have been supported by the Austrian Science Foundation (Project Nos. P 10269 and P 10947) and Conicet (Res. No. 811). Moreover, L.K. and P.F. thank the Swiss National Science Foundation for financial support. O.T. and J.S. are members of the Conicet of Argentina. We are grateful to Dr. E. Alleno and Dr. C. Godart, CNRS Meudon, for their assistance with the L_{III} spectra.

[1] E. Bauer, R. Hauser, E. Gratz, D. Gignoux, D. Schmitt, and J. G. Sereni, J. Phys. Condens. Matter **4**, 7829 (1992); E. Bauer, K. Payer, R. Hauser, E. Gratz, D. Gignoux, D. Schmitt, N. Pillmayr, and G. Schaudy, J. Magn. Magn. Mater. **104-107**, 651 (1992).

[2] E. Bauer, Le Taun, R. Hauser, E. Gratz, T. Holubar, G. Hilscher, H. Michor, W. Perthold, C. Godart, E. Alleno, and K. Hiebl, Phys. Rev. B **52**, 4327 (1995).

[3] E. Bauer, E. Gratz, L. Keller, P. Fischer, and A. Furrer, Physica B **186-188**, 608 (1993).

[4] J. Schefer, P. Fischer, H. Heer, A. Isacson, M. Koch, and R. Thut, Nucl. Instrum. Methods Phys. Res. A **288**, 477 (1990).

[5] R. Bachmann, F. J. DiSahro, Jr., T. A. Geballe, R. L. Greene, R. E. Howard, C. N. King, A. C. Kirsch, K. N. Lee, R. E. Schwall, H. U. Thomas, and R. B. Zubeck, Rev. Sci. Instrum. **43**, 205 (1972).

[6] A. Eiling and J. Schilling, J. Phys. F **11**, 623 (1981).

[7] A. Iandelli and A. Palenzona, J. Less-Common Met. **25**, 333 (1971).

[8] P. Bonville and E. Bauer, J. Phys. Condens. Matter **8**, 7797 (1996).

[9] B. Sales and D. Wohlleben, Phys. Rev. Lett. **35**, 1240 (1975).

[10] K. D. Schotte and U. Schotte, Phys. Lett. **55A**, 38 (1975); C. D. Bredl, F. Steglich, and K. D. Schotte, Z. Phys. B **29**, 327 (1978).

[11] J. D. Thompson, in *Frontiers in Solid State Sciences*, edited by L. C. Gupta and M. S. Multani (World Scientific, London, 1993), Vol. 2, p. 107.

[12] D. Cornut and B. Coqblin, Phys. Rev. B **5**, 4541 (1972).

[13] M. Nicolas-Francillon, A. Percheron, J. C. Achard, O. Gorochov, B. Cornut, D. Jerome, and B. Coqblin, Solid State Commun. **11**, 845 (1972).

[14] A. C. Hewson, *The Kondo Problem to Heavy Fermions*, Cambridge Studies in Magnetism, Vol. 2 (Cambridge University Press, Cambridge, England, 1993).

[15] E. Bauer, Adv. Phys. **40**, 417 (1991).

[16] G. Wortmann (private communication).

[17] H. von Löhneysen, J. Magn. Magn. Mater. **157-158**, 605 (1996), and references cited therein.

[18] M. A. Continentino, Z. Phys. B **101**, 197 (1996).

[19] E. Miranda, V. Dobrosavljevic, and G. Kotliar, J. Phys. Condens. Matter **8**, 9871 (1996).

[20] T. Moriya and T. Takimoto, J. Phys. Soc. Jpn. **64**, 960 (1995).

[21] B. Bogenberger and H. von Löhneysen, Phys. Rev. Lett. **74**, 1016 (1995).